Published in final edited form as:
Dev Neurobiol. 2014 January ; 74(1): . doi:10.1002/dneu.22120.

Distinct roles of *Drosophila cacophony* and *Dmca1D* Ca^{2+} channels in synaptic homeostasis: Genetic interactions with *slowpoke* Ca^{2+}-activated BK channels in presynaptic excitability and postsynaptic response

Jihye Lee[#1,3], **Atsushi Ueda**[#2], and **Chun-Fang Wu**[1,2,#]

[1]Interdisciplinary Program in Neuroscience, The University of Iowa, Iowa City, IA 52242, USA

[2]Department of Biology, The University of Iowa, Iowa City, IA 52242, USA

[3]Department of Oral Pathology, School of Dentistry, Pusan National University, Yangsan-Si, Kyoungsangnam-Do, 626-870, Korea

[#] These authors contributed equally to this work.

Abstract

Ca^{2+} influx through voltage-activated Ca^{2+} channels and its feedback regulation by Ca^{2+}-activated K^+ (BK) channels is critical in Ca^{2+}-dependent cellular processes, including synaptic transmission, growth and homeostasis. Here we report differential roles of *cacophony* (Ca_V2) and *Dmca1D* (Ca_V1) Ca^{2+} channels in synaptic transmission and in synaptic homeostatic regulations induced by *slowpoke* (*slo*) BK channel mutations. At *Drosophila* larval neuromuscular junctions (NMJs), a well-established homeostatic mechanism of transmitter release enhancement is triggered by experimentally suppressing postsynaptic receptor response. In contrast, a distinct homeostatic adjustment is induced by *slo* mutations. To compensate for the loss of BK channel control presynaptic Sh K^+ current is upregulated to suppress transmitter release, coupled with a reduction in quantal size. We demonstrate contrasting effects of *cac* and *Dmca1D* channels in decreasing transmitter release and muscle excitability, respectively, consistent with their predominant pre- vs. post-synaptic localization. Antibody staining indicated reduced postsynaptic GluRII receptor subunit density and altered ratio of GluRII A and B subunits in *slo* NMJs, leading to quantal size reduction. Such *slo*-triggered modifications were suppressed in *cac;;slo* larvae, correlated with a quantal size reversion to normal in double mutants, indicating a role of *cac* Ca^{2+} channels in *slo*-triggered homeostatic processes. In *Dmca1D;slo* double mutants, the quantal size and quantal content were not drastically different from those of *slo*, although *Dmca1D* suppressed the *slo*-induced satellite bouton overgrowth. Taken together, *cac* and *Dmca1D* Ca^{2+} channels differentially contribute to functional and structural aspects of *slo*-induced synaptic modifications.

Keywords

Synaptic transmission; *cacophony* (Ca_V2); *Dmca1D* (Ca_V1); *slowpoke* (BK); synaptic homeostasis; EJPs; mEJPs; spontaneous vesicle release; larval neuromuscular junction (NMJ)

Correspondence to: Chun-Fang Wu.
[#]**Corresponding Author**:

INTRODUCTION

Homeostasis of neuronal excitability and synaptic strength has been well demonstrated in a number of defined neural circuits in invertebrate species (Turrigiano et al., 1995; Marder et al., 1996; Stewart et al., 1996) and in vertebrates (Plomp et al., 1992; Turrigiano, 2004 for review). However, the underpinning molecular mechanisms still await further exploration. In *Drosophila* larval neuromuscular junctions (NMJs), a striking phenomenon was reported in an earlier study, in which nearly-intact excitatory junctional potential (EJP) sizes are observed despite the fact that the number of synaptic boutons or releasing sites are greatly decreased by Fasciclin II mutations (Stewart et al., 1996). Similar upregulation of transmitter release is observed when the miniature EJP (mEJP) amplitude, the quantal size, is diminished by mutations (Peterson et al., 1997; DiAntonio et al., 1999) and pharmacological blockade of glutamate receptors (Frank et al., 2006), or by forced expression of K^+ channels in postsynaptic muscle cells (Paradis et al., 2001). A bone morphogenic protein (BMP) -mediated signaling mechanism has been discovered in follow-up investigations (Frank et al., 2009) to mediate this homeostatic adjustment that is triggered trans-synaptically to increase the number of vesicles released or the quantal content. This line of research has established a clear example of synaptic homeostasis in a genetic model system, in which cellular mechanisms of identified or novel signaling pathway can be further studied (Frank et al., 2006; Dickman and Davis 2009; Frank et al., 2009; Müller et al., 2012).

One conclusion derived from the above studies is that this homeostatic regulation depends on increased presynaptic Ca^{2+} influx (Frank et al., 2006, 2009; Müller et al., 2012). We have previously reported a surprising homeostatic regulation of synaptic strength of a different nature in *slo* mutants, in which synaptic transmission appears largely intact at physiological Ca^{2+} concentrations, despite the dysfunction in Ca^{2+}-activated K^+ channels (BK), a major feedback repolarizing force to terminate Ca^{2+} influx for transmitter release (Lee et al., 2008). The homeostatic adjustments to maintain nearly normal EJP sizes involve modifications of both pre- and post-synaptic properties. Specifically, presynaptic Shaker (Sh) K^+ current is upregulated to compensate for the reduced repolarizing BK currents. Suppression of Sh K^+ current in *slo* mutants by 4-AP immediately leads to explosive EJPs. Moreover, a change in postsynaptic glutamate receptor subunit compositions leads to reduced quantal size. These two adjustments contribute to the restoration of transmission levels in *slo* mutants (Lee et al., 2008).

In a separate study, we described a striking overgrowth of satellite boutons in *slo* larval NMJs (Lee and Wu, 2010), in which distinct patterns of genetic interactions of *slo* BK channels with two types of Ca^{2+} channels, separately encoded by *cac* and *Dmca1D*, dictate the expression of this satellite synaptic outgrowth. Therefore, it is of interest to determine whether such distinct couplings of Cac and Dmca1D channels with BK channels also play separate roles in homeostatic regulations of synaptic transmission in *slo* mutants (Lee et al., 2008). In the present study, physiological alterations in single and double mutants of *cac*, *Dmca1D*, and *slo* demonstrate distinct patterns of functional interactions between *slo*-encoded BK channels with *cac*- and *Dmca1D*-encoded Ca^{2+} channels. The findings implicate differential involvements of Cac and Dmca1D channels in homeostatic regulation of synaptic function and structure.

METHODS

Fly stocks

The fly stocks used in this study have been previously described (Lee et al., 2008; Lee and Wu, 2010) and include: wild type (WT) Canton-S (CS) and when specified in some cases,

Oregon-R (OR); K^+ channel mutants, *slowpoke* (*slo*) (*slo*^{1}, *slo*^{98}, *slo*^{1}/*slo*^{4}, and *slo*^{98}/*slo*^{4}); Ca^{2+} channel mutants, *cacophony* (*cac*) (*cac*^{S} and *cac*^{NT27}) and *Dmca1D* (*Dmca1D*^{AR66}); double mutant combinations, *cac;;slo* (*cac*^{S}*;;slo*^{1}, *cac*^{S}*;;slo*^{98}, and *cac*^{S}*;;slo*^{4}) and *Dmca1D;slo* (*Dmca1D*^{AR66}*;slo*^{1} and *Dmca1D*^{AR66}*;slo*^{98}). Data collected from different alleles of *slo* and their combinations with *cac*^{s} and *Dmca1D*^{AR66} indicate similar physiological phenotypes. Thus, results from the different alleles are combined in analysis to increase statistical power. All these stocks were raised in the presence of conventional fly medium and maintained at room temperature.

Preparations and Electrophysiology

Preparation of wandering third instar larvae and intracellular recordings of excitatory junctional potentials (EJPs) and miniature EJPs (mEJPs) were performed as described previously (Lee et al., 2008). Briefly, evoked EJPs upon segmental nerve stimulation were recorded from muscle 6 or 7 in abdominal segments 3 through 6, mostly from 4th and 5th segments, in HL3.1 saline (Feng et al., 2004) containing Ca^{2+} at specified concentrations. The correction procedure for nonlinear summation of synaptic potential (Martin, 1955; Lee et al., 2008) was applied for EJP amplitude comparison. Miniature EJPs (mEJPs) at the resting membrane potential more negative than −60 mV were analyzed for their frequency and amplitude (MiniAnalysis, Synaptosoft Inc., Fort Lee, NJ, USA). Quantal content was calculated by dividing the mean EJP amplitude (corrected for nonlinear summation) by the mean mEJP amplitude at the same NMJs. All EJP data were collected using CLAMPEX and FETCHEX (version 5.5, Molecular Devices Corporation, Sunnyvale, CA, USA) and analyzed using CLAMPFIT (version 6.0, Molecular Devices Corporation) and Origin software (version 6.0, OriginLab Corporation, Northampton, MA, USA). Selective blockade of Sh K^+ channel function was achieved by a bath application of 4-AP (0.2 mM, Sigma-Aldrich Corp., St. Louis, MO, USA) at least for 2 min before data collection.

Direct electrotonic stimulation of the nerve terminal

In order to examine the Ca^{2+} influx-dependent excitability in the nerve terminal, transmitter release was evoked by direct electrotonic stimulation of the nerve terminals after nerve action potentials were blocked with 3 μM TTX (Ganetzky and Wu, 1982). Depolarization (1 ms) was applied through the suction electrode near the nerve entry point in the proximity of motor terminals to increase the effectiveness of electrotonic stimulation. With increasing stimulus intensity, electrotonically evoked EJCs gradually increased in amplitude until a saturation level was reached. Under this condition, further amplification of the Ca^{2+}-supported excitability in presynaptic axon terminals can be achieved by removing the repolarization force using K^+ channel blockers 4-AP (4-Aminopyridine, 200 μM) and TEA (Tetraethylammonium, 20 mM). As a result, sustained presynaptic Ca^{2+} action potentials leads to strikingly prolonged EJPs, with durations up to a few seconds (Ganetzky and Wu, 1982, 1983; Ueda and Wu, 2009). In order to obtain consistent results, we adjusted the stimulus voltage to the level where these plateau EJPs were triggered most frequently.

Muscle current injection

Muscle action potentials were triggered by depolarizing current injection into muscle cells bathed in the HL3.1 saline containing 2 mM Sr^{2+}, 0 mM Ca^{2+}, and 16 mM Mg^{2+}. *Drosophila* larval muscles normally do not display overshooting Ca^{2+} spikes. However, depolarizing current injection with saline containing Sr^{2+} can readily trigger muscle action potentials since Sr^{2+} is a more effective charge carrier through the Ca^{2+} channels, suppressing Ca^{2+} channel inactivation and partially blocking K^+ channels (Hille, 2001). The Ca^{2+}-free saline (nominally 0 mM) also helped to suppress muscle contraction. The high

Mg^{2+} concentration (16 mM) compensates for the decreased surface charge screening effect due to the absence of Ca^{2+}.

Pharmacological agents

Tetrodotoxin (TTX) was obtained from Sigma (St. Louis, MO, USA). Charybdotoxin (ChTX) was purchased from Alomone Labs (Jerusalem, Israel).

Immunohistochemistry and Image analysis

Wandering larvae at the third instar stage were fixed and prepared as described (Lee et al., 2008). Briefly, dissected larvae were fixed with either 100% ice-cold methanol for 5 min for immunostaining with both anti-DGluRIIA and -DGluRIIB antibodies, otherwise with 3.7% formaldehyde in phosphate buffer saline for 20 min. The primary antibodies used include: monoclonal Brp (NC82, 1:50, Developmental Studies Hybridoma Bank (DSHB), Univ. of Iowa) and DGluRIIA antibody (8B4D2, 1:50, DSHB, Univ. of Iowa), and rabbit polyclonal DGluRIIB (1:500) antibody (a generous gift from Dr. A. DiAntonio at Washington Univ., St. Louis). The fluorescent secondary antibodies at 1:250 were obtained from Jackson ImmunoResearch Laboratories (West Grove, PA, USA). The overall structure of NMJs was visualized with FITC-conjugated anti-HRP antibody. For direct comparison of DGluRIIA and DGluRIIB density among different genotypes, all larvae were processed together, treated with the same antibody and washout solutions within individual tubes and washout chambers throughout the procedure.

Images of NMJs on muscles 6/7 from abdominal segments 3 through 4 were collected using Zeiss LSM5 and LSM700 confocal microscopes (Carl Zeiss Microscopy, LLC, One Zeiss Drive, Thornwood, NY, USA) with an oil-immersed 40X objective and analyzed as previously described (Lee et al., 2008). For direct comparison of DGluRII subunit density measurements across genotypes, all larvae in the same batch were subjected to the same settings for exposure and signal detection. The average pixel intensity readings for DGluRIIA and DGluRIIB signals and their ratio (IIA/IIB) from the collapsed Z-stacked images for each genotype were then normalized to the average value from the WT NMJs to facilitate comparisons across different genotypes.

Statistical Analyses

For comparison between two genotypes, a Chi-Square test was carried out as specified in figure legends. For multiple comparison, we used One-way ANOVA followed by multiple comparisons using Fisher's LSD test. *P*-values less than 0.05 was considered to be significantly different. All statistical analyses were performed using Origin software (version 6.0, OriginLab Corporation).

RESULTS

Effects of *cacophony* and *Dmca1D* mutations on Ca^{2+} dependency of synaptic transmission

As described above, it is well established that *cac*-encoded Ca^{2+} channels play an important role in regulating nerve-evoked synaptic responses. However, the role of *Dmca1D*-encoded L-type Ca^{2+} channels in synaptic transmission remains to be documented. Thus, we first compared how *cac* and *Dmca1D* mutations affect synaptic transmission in HL3.1 recording saline. Since the known null alleles of either *cac* or *Dmca1D* mutations are embryonic lethal (Smith et al., 1996; Eberl et al., 1998), the viable alleles of *cac* and *Dmca1D* mutations were used here (cac^S and $Dmca1D^{AR66}$). At 0.2 mM $[Ca^{2+}]_o$, we were able to detect reliable EJP responses upon nerve stimulation in both WT and *Dmca1D* larvae. At lower Ca^{2+} levels, the

response amplitude of these EJPs was more variable, reflecting fluctuation in the number of released quanta. However, there were no significant differences in EJP amplitude between WT and *Dmca1D* [Fig. 1]. In contrast, a drastic reduction in transmitter release was found in all cac^S larvae examined [Fig. 1], with some larvae (2/14) displaying complete response failures, i.e. no quanta released [Data not shown], consistent with the previous reports on a different synaptic preparation (Kawasaki et al., 2000; Kawasaki et al., 2002). As $[Ca^{2+}]_o$ increased, EJP amplitude in both WT and *Dmca1D* larvae was drastically enhanced and reached saturated levels around 1.0 mM of $[Ca^{2+}]_o$. However, EJP amplitude in cac^S mutants remained significantly smaller at physiological $[Ca^{2+}]_o$ [0.5 mM or higher, Fig. 1(B)]. The above observations support the notion that synaptic vesicle release is regulated by Ca^{2+} influx mainly through *cac*-encoded Ca^{2+} channels in the presynaptic terminal.

Effects of *cacophony* and *Dmca1D* mutations on pre and postsynaptic membrane excitability

We examined the effects of *cac* and *Dmca1D* mutations on Ca^{2+}-supported excitability in presynaptic axon terminals, using a previously established protocol of direct electrotonic stimulation of the terminal (Ganetzky and Wu, 1982, 1983; Ueda and Wu, 2009). After silencing Na^+ spikes with TTX, the nerve terminal was depolarized by the electrotonic spread of a stimulus of increased duration, which lead to EJPs of graded amplitudes in response to varying stimulus voltage at WT NMJs (Wu et al., 1978). After removal of the repolarization force by K^+ channel blockers 4-AP and TEA, the EJP response was no longer graded and displayed explosive all-or-none plateau potentials [Fig. 2(A)] due to sustained presynaptic Ca^{2+} spikes (Ganetzky and Wu, 1982; 1983), as first described in the squid giant synapse and the frog neuromuscular junction under similar conditions (Katz and Miledi, 1969ab). As shown in Figure 2, such prolonged plateau EJPs were intact in the majority of *Dmca1D* muscle fibers tested (4 out of 6 muscles, 3 larvae), but were observed in *cac* larvae only in rare occasions [2 out of 8 muscles, 3 larvae; Fig. 2(A)]. Our result from the hypomorphic alleles (cac^s, see Methods) is consistent with the previous imaging study on the same *cac* mutants, showing a decrease in Ca^{2+} influx-induced fluorescence signal (Macleod et al., 2006).

We also examined the Ca^{2+}-supported excitability in postsynaptic muscle membrane using the current injection technique (see Methods). As previously shown, *Drosophila* larval muscles normally do not display overshooting Ca^{2+} spikes unless the repolarizing K^+ currents are suppressed by K^+ channel blockers, such as TEA, or by using Sr^{2+} as the charge carrier, which also blocks K^+ channels (Singh and Wu, 1990; Ueda and Wu, 2006). We found that by replacing Ca^{2+} with Sr^{2+}, depolarizing current pulses (700 ms) evoked an overshooting spike potential followed by a sustained plateau lasting hundreds of milliseconds in both WT and *cac* larval muscles [Fig. 2(B)]. In contrast, we did not observe sustained plateau potentials in $Dmca1D^{AR66}$, a hypomorph (Eberl et al., 1998), which was able to produce only brief overshooting spikes (10 ms). This is consistent with the previous finding that postsynaptic muscle Ca^{2+} currents are predominantly mediated by dihydropyridine-sensitive Ca^{2+} channels (Gielow et al., 1995).

Effects of *cac* and *Dmca1D* on *slo*-induced synaptic homeostasis in double mutants

As described above, the known null alleles of either *cac* or *Dmca1D* mutations are embryonic lethal (Smith et al., 1996; Eberl et al., 1998), therefore the viable alleles of *cac* and *Dmca1D* mutations were used here (cac^S and $Dmca1D^{AR66}$). Despite an undetermined amount of residual currents that could remain in these hypomorphic mutant alleles, their profound functional consequences are clearly indicated by the severe EJP reduction in cac^S [Fig. 1] and in the striking genetic interactions of both cac^S and $Dmca1D^{AR66}$ with *slo* in synaptic morphology previously described (Lee and Wu, 2010). These more commonly used

cac and *Dmca1D* mutant alleles were thus employed in double mutant experiments described below. Another viable *cac* allele, cac^{NT27}, displayed similar phenotypes of decreased EJP responses [Data not shown].

In *Dmca1D;slo* double mutants, there were only a few viable *Dmca1D;slo* third-instar larvae, few of which succeeded in eclosion, as expected from the severe lethality of *Dmca1D* mutants (Eberl et al., 1998). Surprisingly, the EJP amplitude in viable *Dmca1D;slo* escapees was comparable to that of *slo* single mutants, regardless of $[Ca^{2+}]_o$ levels [Fig. 3(B); see also Fig. 1]. In other words, Ca^{2+}-dependent homeostatic adjustment of EJP amplitude in *slo* mutants was apparently undisturbed in *Dmca1D;slo* double mutants. Thus, functional interaction between *Dmca1D*-encoded Ca^{2+} and *slo* BK channels in other cellular compartments or cell types may be responsible for the lethality of the double mutants.

In contrast to *Dmca1D*, striking interactions between *cac* and *slo* led to severely impaired synaptic transmission and an apparent suppression of *slo*-induced homeostatic regulation of EJP size [Fig. 3(C)]. Similar to *Dmca1D;slo* double mutants, several *cac;;slo* combinations of hypomorphic alleles are largely pupal lethal, while double mutants with the slo^4 null allele were nearly larval lethal. Viable hypomorphic double-mutant larvae were smaller in size, and the adult escapees exhibited an uncoordinated walking behavior, abnormal wing posture, poor flight ability, and short lifespan [Data not shown].

In addition to these developmental and behavioral abnormalities, we found a drastically reduced EJP amplitude in *cac;;slo* double mutants. At lower external Ca^{2+} concentrations (0.2 mM of $[Ca^{2+}]_o$), complete synaptic failures (no detectable synaptic responses upon nerve stimulation) occurred in the majority of preparations [8/13; Fig. 3(A,C)], with only a few larvae displayed occasional EJP responses upon repetitive nerve stimulation [Data not shown]. Furthermore, there was no indication of *slo*-induced homeostatic responses in *cac;;slo*, i.e. restoration of EJP amplitude to the WT level at physiological $[Ca^{2+}]_o$, but rather, a further decrement of EJP amplitudes compared to either single mutant [Fig. 3(A,C)]. These findings illustrate the important functional coupling between *cac*-encoded N-type Ca^{2+} and *slo*-encoded BK channels in maintaining synaptic function and homeostasis. It is surprising that weakening of repolarization due to *slo* BK channel disruption could actually result in further EJP amplitude reduction in *cac;;slo* double mutants as compared to *cac* single mutants, indicating altered developmental regulation of the transmitter release mechanism. To test this notion, we employed a highy specific antagonists of BK channels, charybdotoxin (ChTx, 50 nM, Elkins et al., 1986, Singh and Wu, 1990) to eliminate acutely Slo BK K^+ currents in the *cac* mutant background. Consistently, reduction in EJP amplitude in *cac;;slo* could not be mimicked by the acute blockade of Slo BK current by ChTx in *cac* mutants, confirming a long-term regulatory effect conferred by *cac*-*slo* interaction [Table 1].

Effects of *cac* and *Dmca1D* on *slo*-induced homeostatic regulation of postsynaptic quantal response

Spontaneous miniature EJPs (mEJPs) represent the postsynaptic quantal response to the randomly occurring unitary fusion event of presynaptic transmitter vesicles. The amplitude of these events in part reflects postsynaptic receptor properties or density. We have previously demonstrated that homeostatic adjustment of synaptic strength in *slo* mutants is partially achieved via a reduction in quantal size (Lee et al., 2008). We thus examined the consequences of interaction between Slo and pre- vs. post-synaptic Ca^{2+} channels in single and double mutants by monitoring these quantal events.

We found that although *cac* mutations caused a moderate, but significant, reduction in mEJP amplitude, intriguingly, *cac;;slo* double mutants displayed significantly greater mEJP amplitudes compared to the reduced mEJP size in *slo* single mutants, essentially restored to

the WT-level quantal size [Fig. 4(A,B)]. This observation again supports a major role of *cac* in *slo*-induced homeostatic reduction in postsynaptic quantal response. We found that a similar trend of quantal size increase might also be present in *Dmca1D;slo* double mutants although it did not reach a statistically significant level [Fig. 4(A,B)].

We further examined the rate of spontaneous vesicle fusion events in presynaptic terminals and discovered unexpected alterations associated with *Dmca1D*, *cac*, and *slo* interactions in different manners. Interestingly, among the three single mutants, mEJP frequency was significantly reduced only in *Dmca1D* mutants compared to WT [Fig. 4(C), $P<0.01$, WT vs. *Dmca1D*; see also examples of mEJPs in Fig. 4(A)]. Given its postsynaptic localization at the NMJ, a transsynaptic signaling mechanism may be involved to exert the *Dmca1D* mutational effects on the presynaptic release process. When *Dmca1D* was combined with *slo* in double mutants, the frequency of mEJPs was not different from that of *slo* or WT larvae [Fig. 4(C)]. Unexpectedly, a stronger genetic interaction between *cac* and *slo* was indicated by a drastic increase in spontaneous mEJP frequency in *cac;;slo* double mutants, clearly surpassing that in WT and either single mutant [Fig. 4(C); see also examples of mEJP traces in Fig. 4(A)].

Together with the restoration of quantal size, the contrasting effects of combining *Dmca1D* and *cac* with *slo* on the mEJP frequency suggest different modes of regulation. Apparently, a trans-synaptic molecular mechanism exists to confer the *Dmca1D* interaction with *slo* vs. a presynaptic mechanism for *cac* interaction with *slo* to produce the observed regulations on the presynaptic release efficacy.

Effects of *cac* mutations on presynaptic active zone distributions and postsynaptic glutamate receptor properties

As described above, our data demonstrate alterations in the size and frequency of quantal events induced by *cac* mutations in combinations with *slo* [Fig.4]. Thus, we performed immunostaining of pre- and post-synaptic molecular markers to probe the synaptic components responsible for quantal size determinations and transmitter release regulations. We employed the antibodies specific for the presynapyic active zone protein Bruchpilot and the postsynaptic receptor subunits GluRIIA and B. Our results from NC82 staining [Fig. 5] clearly demonstrated that Bruchpilot proteins in the active zones remained abundant in *cac;;slo* double mutants. The NMJ structure visualized with anti-HRP immunoreactivity (see Methods) also indicated that the general morphology of the nerve-terminal arbors in double mutants was not drastically altered, with nearly normal numbers of synaptic boutons and Bruchpilot reactive puncta, although there were still abundant satellite boutons (cf. Lee & Wu, 2010). However, the modification in satellite bouton numbers could not be the cause of enhanced spontaneous mEJP frequencies in *cac;;slo* because a similar level of satellite bouton overgrowth occurred in *slo* without a corresponding increase in spontaneous mEJPs [Fig. 4]. The resolution of our NC82 immunostaining images does not allow firm quantitative conclusions on potentially altered number or intensity of active zone immuno reactivity. Future ultrastructural analysis is required to examine whether alterations of the active zone are responsible for the drastically decreased release efficacy (or low quantal content) indicated by the diminished *cac;;slo* EJPs.

We have previously reported that the regulation of quantal event amplitude, i.e. mEJPs, may in part involve modification in postsynaptic receptor composition or density, which contributes to homeostatic regulation of synaptic strength in the absence of Slo BK channel activities (Lee et al. 2008). Importantly, our data indicate clear restoration of quantal size in *cac;;slo* mutants, in contrast to reduced mEJP amplitude in *slo* single mutants. Thus, we performed immunohistochemical analysis of postsynaptic glutamate receptor properties in WT as well as *slo*, *cac*, and *cac;;slo* mutants. For direct comparisons of receptor density, we

took precautions to obtain more quantitative results from simultaneous GluRIIA and GluRIIB immunostaining. The larval preparations from different genotypes were processed together and went through the staining procedure in the same chamber. Figure 6 shows a clear decrease in GluRIIA and GluRIIB immunoreactivity in *slo*, which may underlie the reduced mEJP size in *slo*. Furthermore, there was a reduced GluRIIA/GluRIIB (IIA/IIB) ratio because of the more drastic reduction in IIA than IIB [Fig. 6], in line with our observation that also demonstrates a positive correlation between the receptor subtype ratio (IIA/IIB) and quantal size (Lee et al., 2008). Significantly, the postsynaptic receptor density and IIA/IIB ratio were restored to nearly-WT levels in *cac;;slo* double mutants [Fig. 6], consistent with the restoration of quantal size to the WT mEJP level in the electrophysiological recordings [Fig. 4(B)]. Taken together, these observations further confirm a major role of *cac* in *slo*-induced homeostatic reduction.

Effects of acute pharmacological blockade of *slo* BK channels on quantal size

To gain insight into the time scale of the potential homeostatic mechanisms, it is important to establish whether such phenotype could be mimicked by acute blockade of functional interaction between these two channel types. We applied ChTx (50 nM) to eliminate acutely Slo BK K^+ currents in the *cac* mutant background. As shown in Figure 7, the ChTx treatment in two independent alleles of *cac* mutants failed to reproduce the phenotypes of *cac;;slo* in the upregulation of the frequency of mEJPs [Fig. 7, cac^S;cac^{NT27}, Data not shown]. Furthermore, there was no significant change in either mEJP or EJP amplitude following an application of ChTx in *cac* mutants [Fig. 7(C) and Table 1]. Taken together, these results indicate that disrupted coupling between presynaptic Ca^{2+} and BK channels can lead to an altered development of synaptic vesicle pool distribution or release mechanism, leading to the striking increase in spontaneous fusion events.

Effects of *cac* and *Dmca1D* on *slo*-induced homeostatic upregulation of presynaptic 4-AP-sensitive Sh I_A

The strong synergistic effects of *cac* and *slo* mutations on mEJP and EJP properties prompted us to seek indications for a role of *cac* Ca^{2+} channels in another prominent feature of *slo*-induced synaptic homeostatic responses, i.e. upregulation of presynaptic Shaker (Sh) I_A in compensation for the loss of repolarizing Slo BK current. As previously demonstrated, 4-AP treatment produces a striking effect on *slo* NMJs, in which supernumerary or prolonged EJPs of increased amplitudes can be evoked by a single nerve stimulus (Lee et al., 2008). Such multiple EJPs suggested presynaptic hyperexcitability upon 4-AP blockade of upregulated Sh I_A, a consequence of eliminating both voltage-activated I_A and Ca^{2+}-activated BK, causing motor axon terminal repetitive firing that was not observed in WT larvae under the same treatment [Fig. 8]. We examined how this feature is further modified by *cac* and *Dmca1D* mutations in double mutants at a low Ca^{2+} level (0.2 mM, well below saturation levels of EJPs in order to optimize the sensitivity of detection).

Importantly, despite drastically decreased transmission compared to *slo*, *cac* single mutants displayed certain aspects similar to *slo* larvae following 4-AP treatment, i.e., a tendency of producing broadened and supernumerary EJPs not found in WT larvae [Fig. 8]. It is likely that reduced Ca^{2+} current in *cac* mutants would result in weakened activation of Slo (BK) K^+ current, thus indirectly trigger *slo*-like upregulation of Sh I_A. Our previous voltage-clamp studies show that reduction in Slo current in cultured *cac* neurons is compensated for by a Sh I_A increase to maintain a nearly constant total K^+ conductance (Peng and Wu, 2007). Thus, a similar compensatory mechanism may be activated in *cac* NMJs. Along with reduced Slo current, 4-AP blockade of upregulated Sh I_A in *cac* could lead to the phenotype observed here [Fig. 8].

The increment of EJP amplitude in *cac;;slo* after 0.2 mM 4-AP treatment was clearly to a lesser extent as compared to that in either single mutants [Fig. 8]. However, the proportional increase in quantal content could be in fact higher than WT because of the much suppressed release in *cac;;slo* before 4-AP treatment [Fig. 3 and Fig. 8; compare *cac;;slo* with *cac* or *slo*]. Notably, *cac;;slo* mutants, in some rare cases, were capable of generating supernumerary EJPs with further increment of 4-AP [from 0.2 to 2 mM; Data not shown]. These results suggest that *slo*-induced homeostatic upregulation of presynaptic Sh I_A might still be present in *cac;;slo*, albeit to a lesser extent.

In contrast to *cac;;slo*, 4-AP-treated *Dmca1D;slo* double mutants displayed supernumerary EJPs similar to *slo* [Data not shown], indicating that *slo*-induced enhancement of 4-AP sensitivity could occur with disrupted *Dmca1D*-encoded postsynaptic Ca^{2+} channels.

The highly nonlinear nature of supernumerary and prolonged EJPs caused by 4-AP treatment precludes quantitative estimates of Sh I_A upregulation from dosage-dependent measurements. However, qualitative assessments of the increase of EJP sizes after 4-AP treatment clearly indicate that the 4-AP effects were greatest on *slo* and *cac*, less on *cac;;slo*, and least on WT.

DISCUSSION

In this study, we extended our previous findings to investigate the roles of two identified Ca^{2+} channels in *slo* mutation-induced homeostatic regulation of presynaptic transmitter release and postsynaptic quantal response. We first characterized the functional roles of the *cac*- and *Dmca1D*-encoded Ca^{2+} channels in membrane excitability and transmitter release control at the larval NMJ [Fig. 1 and Fig. 2]. In different double mutant combinations with *slo*, we further determined the effects of *cac* and *Dmca1D* mutations on *slo*-induced homeostatic regulation in the pre- and post-synaptic compartments. Figure 9 summarizes several observed features of synaptic homeostasis that have been found in mutants of *slo* BK channels in the previous and present studies, i.e. cAMP-dependent upregulation of presynaptic Sh I_A, postsynaptic modification of glutamate receptor composition, and synaptic bouton growth (Lee et al., 2008; Lee and Wu, 2010), as well as further modifications of these phenotypes by *cac* and *Dmca1D* in *cac;;slo* and *Dmca1D;slo* double mutants. Our results indicate separate roles of two distinct Ca^{2+} channels in *slo*-induced homeostatic regulatory processes, with *cac* and *Dmca1D* preferentially affecting synaptic function and structure, respectively [Fig. 9]. Our work also revealed several unexpected chronic effects of *cac* and *Dmca1D* mutations on both quantal size and spontaneous mEJP discharge frequencies [Fig. 4 and Fig. 7].

Types of voltage-gated Ca^{2+} channels in *Drosophila*

The influx of Ca^{2+} via voltage-activated Ca^{2+} channels influences a diversity of cellular function and growth processes. In vertebrates, subtypes of Ca^{2+} channels, e.g. L, N, P, Q, and R types, vary in threshold, inactivation, and pharmacological properties, and are identified with distinct functional domains of the α_1 pore-forming subunit (Tsien et al., 1988; Catterall, 2000; Ertel et al., 2000). In *Drosophila*, the existence of distinct Ca^{2+} channel types in neurons and muscles has been suggested by differences in sensitivity to the various Ca^{2+} channel blockers (Pauron et al., 1987; Greenberg et al., 1989; Leung et al., 1989; Pelzer et al., 1989; Leung and Byerly, 1991; Singh and Wu 1999). Subsequent genetic and molecular studies have identified two genes encoding distinct Ca^{2+} channel α_1 subunits; *cac* encodes a subunit that shares sequence similarities to vertebrate N-type Ca^{2+} or Ca_V2 channels (von Schilcher 1976; Smith et al., 1996; Rieckhof et al., 2003), and *Dmca1D* encodes a subunit homologous to rabbit brain L-type or Ca_V1 channels (Zheng et al., 1995). Our report here further extends the functional characterization of these two channels in

larval nerve and muscle. A third class of Ca^{2+} channel α_1 subunits of low voltage-activated (LVA) Ca_V3 channels has been inferred from sequence homology of a gene, *Dmca1G* (Littleton and Ganetzky, 2000). Further, patch-clamp studies have demonstrated the existence of a LVA current in adult thoracic motor neuron somata (Worrell and Levine, 2008; Ryglewski et al., 2012) and in cultured embryonic neuroblasts (Peng and Wu, 2007). However, it remains to be determined whether the *Dmca1G*-encoded channel also plays a role in regulating NMJ function or structure. Another gene, *straightjacket*, is known to encode an auxiliary subunit for the *cac* Ca^{2+} channel (Dickman et al., 2008; Ly et al., 2008). This α_2-delta subunit is important for localization of Cac channels to trigger synaptic transmission (Dickman et al., 2008; Ly et al., 2008) and for regulating synaptic vesicle recycling (Kuromi et al., 2010). The α_2-delta subunit can conceivably modify *slo*-induced synaptic homeostasis as well.

Importance of intact *cac* Ca^{2+} channels in *slo*-induced regulation of mEJP and EJP amplitudes

One important feature of *slo*-induced synaptic homeostasis is to reduce the quantal size. We found normal density and subunit composition of postsynaptic DGluRII [Fig. 6] in correlation with normal size of mEJPs [Fig. 4] in *cac;;slo* double mutants. This result demonstrates that Cac channel function is required for the *slo* -induced down regulation of mEJP amplitude [Fig. 9]. In fact, a central role of Cac channels has been established in a different form of synaptic homeostatic regulation upon perturbations of postsynaptic glutamate receptor activities (Petersen et al., 1997; Frank et al., 2006; Frank et al., 2009). In these studies, reducing quantal size by philanthotoxin (PhTx) or *dGluRIIA* mutations leads to homeostatic increase in presynaptic neurotransmitter release, to restore synaptic strength. Such homeostatic responses are suppressed by *cac* mutations affecting $Ca_{V2.1}$ (Frank et al., 2006; Frank et al., 2009).

Although the exact mechanisms remain unknown, the *slo*-induced quantal size adjustment may involve trans-synaptic signaling to allow presynaptically localized Cac channels to confer modification of *slo*-induced adjustment of postsynaptic receptor density and composition [Fig. 7]. One possibility is that the severe reduction in the EJP size at *cac;;slo* NMJs reflect drastically decreased vesicle release, which may limit the discharge of unknown factors stored along with the excitatory neurotransmitter glutamate. For example, neuropeptides may be co-released with transmitter during exocytosis. Recent studies have implicated spontaneous vesicle release as a part of molecular mechanisms to regulate synaptic strength during activity-dependent synaptic plasticity in *Aplysia* cultures (Jin et al., 2012a; Jin et al., 2012b).

Nerve-evoked and spontaneous vesicle release in single and double mutants

One interesting and unexpected finding is a clear effect of interaction between *cac* and *slo* on the spontaneous discharge of synaptic vesicles. Although neither *cac* nor *slo* single mutants showed altered mEJP frequencies, the double mutants displayed a striking increase in the rate of spontaneous mEJPs [Fig. 4]. This interaction is likely to be localized to the presynaptic site to influence spontaneous vesicle release. Our attempt of immuno-chemical staining against the active zone protein Bruchpilot [Brp; recognized by NC82 antibodies, Fig. 5] failed to detect obvious changes in numbers of active zones. Future electron microscopy observations will be required to examine whether more abundant synaptic vesicles or altered proportion of vesicle pools exist near release sites and other subcellular locations (Sudhof, 2004) at *cac;;slo* larval NMJs.

Another notable non-additive interaction between *cac* and *slo* mutations is indicated by the unusually small EJP size in the double mutants. Quantal content deduced from mean EJP

and mEJP amplitudes was decreased in *cac* larvae, but was even more drastically reduced in *cac;;slo* double mutants (nearly to the level of complete transmission failure at the lower Ca^{2+} levels, 0.2 mM), indicating further suppression of presynaptic neurotransmitter release [Fig. 3; 9.57±1.72 mV in WT *vs.* 0.16±0.16 mV in *cac;;slo*]. This severely suppressed vesicle release could in principle be caused by either a further decrease in Ca^{2+} influx through Cac channels or a further increase in *slo*-induced Sh I_A upregulation. However, our 4-AP treatment experiments do not support a striking upregulation of Sh I_A. Whether Ca^{2+} influx might be further reduced by the loss of both Cac Ca^{2+} and Slo BK channel activities in mutants remains to be addressed.

Importance of intact *Dmca1D* Ca^{2+} channels in *slo*-induced morphological modifications

Our data indicate that unlike *cac* mutations, altered Dmca1D function did not exhibit clear modifications of physiological aspects of *slo*-induced synaptic homeostasis, including quantal size reduction and ShIA upregulation. This is in contrast to the previous report that a *slo*-induced, cAMP-dependent aberrant growth of satellite boutons is suppressed in *Dmca1D;slo* double mutants, but not in *cac;;slo* double mutants (Lee and Wu, 2010). This interaction leads to abundant satellite boutons and likely involves postsynaptic functional coupling of *Dmca1D* Ca^{2+} and *slo* BK channels to achieve this trans-synaptic effect on bouton growth regulation [Fig. 9]. As previously shown, Ca^{2+}/calmodulin-activated *rut* adenylyl cyclase (AC) is required for Sh I_A upregulation and satellite bouton overgrowth in *slo* (Lee et al., 2008; Lee and Wu, 2010). Conceivably, presynaptic and postsynaptic Ca^{2+} influx can contribute to the activation of rut AC and the initiation of cAMP cascade [Fig. 9].

Recently, synpatotagmin IV (Syt4), a potential Ca^{2+} sensor for postsynaptic release of retrograde signaling molecule, has been implicated in an increase in presynaptic spontaneous vesicle release following a tetanic nerve stimulation at embryonic NMJs in *Drosophila* (Yoshihara et al., 2005; Barber et al., 2009). It will be interesting to determine whether Dmca1D channels provide Ca^{2+} sources for activating Syt4-dependent retrograde signaling involved in trans-synaptic homeostasis regulations.

It should be noted that *Dmca1D* is also implicated in voltage-clamp studies of the motoneuron soma (Worrell and Levine, 2008). Its role in neuronal homeostatic regulations, especially the *slo*-induced modifications, remains to be investigated. Clearly, the exact mechanisms and additional interacting players in the *slo*-induced synaptic homeostasis require further investigations in the future. At the present time, it is technically challenging to directly determine the properties of normal and altered Ca^{2+} currents at the neuromuscular junction of the mutants in this study. Patch-clamp whole-cell recording from neuronal somata may not obtain the correct picture of the nerve terminals because expression of specific types of Ca^{2+} channels may depend on the cell type and the cellular compartments of the neuron (Peng and Wu, 2007; Worrell and Levine, 2008).

In summary, together with their preferential localization, the distinct interactions between *slo*-encoded BK and two types of Ca^{2+} channels imply their differential roles in synaptic homeostasis. Our results demonstrate the predominant contributions of *cac*- and *Dmca1D*-encoded Ca^{2+} channels to the functional and structural aspects, respectively, of the *slo*-induced synaptic modifications.

Acknowledgments

We thank Dr. T. Littleton for providing fly stocks and Dr. A. DiAntonio for a generous gift of DGluRIIB antibody. This work was supported by NIH GM 088804 to CFW.

REFERENCES

Barber CF, Jorquera RA, Melom JE, Littleton JT. Postsynaptic regulation of synaptic plasticity by synaptotagmin 4 requires both C2 domains. J Cell Biol. 2009; 187:295–310. [PubMed: 19822673]

Catterall WA. Structure and regulation of voltage-gated Ca^{2+} channels. Annu Rev Cell Dev Biol. 2000; 16:521–555. [PubMed: 11031246]

DiAntonio A, Petersen SA, Heckmann M, Goodman CS. Glutamate receptor expression regulates quantal size and quantal content at the Drosophila neuromuscular junction. J Neurosci. 1999; 19:3023–3032. [PubMed: 10191319]

Dickman DK, Kurshan PT, Schwarz TL. Mutations in a *Drosophila* $\alpha_2\delta$ voltage-gated calcium channel subunit reveal a crucial synaptic function. J Neurosci. 2008; 28:31–38. [PubMed: 18171920]

Dickman DK, Davis GW. The schizophrenia susceptibility gene dysbindin controls synaptic homeostasis. Science. 2009; 326:1127–1130. [PubMed: 19965435]

Eberl DF, Ren D, Feng G, Lorenz LJ, Van Vactor D, Hall LM. Genetic and developmental characterization of Dmca1D, a calcium channel alpha1 subunit gene in Drosophila melanogaster. Genetics. 1998; 148:1159–1169. [PubMed: 9539432]

Elkins T, Ganetzky B, Wu CF. A *Drosophila* mutation that eliminates a calcium-dependent potassium current. Proc Natl Acad Sci USA. 1986; 83:8415–8419. [PubMed: 2430288]

Ertel EA, Campbell KP, Harpold MM, Hofmann F, Mori Y, Perez-Reyes E, Schwartz A, Snutch TP, Tanabe T, Birnbaumer L, Tsien RW, Catterall WA. Nomenclature of voltage-gated calcium channels. Neuron. 2000; 25:533–535. [PubMed: 10774722]

Feng Y, Ueda A, Wu CF. A modified minimal hemolymph-like solution, HL3.1, for physiological recordings at the neuromuscular junctions of normal and mutant Drosophila larvae. J Neurogenet. 2004; 18:377–402. [PubMed: 15763995]

Frank CA, Kennedy MJ, Goold CP, Marek KW, Davis GW. Mechanisms underlying the rapid induction and sustained expression of synaptic homeostasis. Neuron. 2006; 52:663–677. [PubMed: 17114050]

Frank CA, Pielage J, Davis GW. A presynaptic homeostatic signaling system composed of the Eph receptor, ephexin, Cdc42, and CaV2.1 calcium channels. Neuron. 2009; 61:556–569. [PubMed: 19249276]

Ganetzky B, Wu CF. Drosophila mutants with opposing effects on nerve excitability: Genetic and spatial interactions in repetitive firing. J Neurophysiol. 1982; 47:501–514. [PubMed: 6279790]

Ganetzky B, Wu CF. Neurogenetic analysis of potassium currents in Drosophila: Synergistic effects on neuromuscular transmission in double mutants. J Neurogenet. 1983; 1:17–28. [PubMed: 6100303]

Gielow ML, Gu GG, Singh S. Resolution and pharmacological analysis of the voltage-dependent calcium channels of Drosophila larval muscles. J Neurosci. 1995; 15:6085–6093. [PubMed: 7666192]

Greenberg R, Streissnig J, Koza A, Devay P, Glossman H, Hall L. Native and detergent-solubilized membrane extracts from Drosophila heads contain binding sites for the phenylalkylamine calcium channel blockers. Insect Biochem. 1989; 19:309–322.

Hille, B. Ion Channels of Excitable Membranes. Sinauer; Sunderland: 2001.

Jin I, Puthanveettil S, Udo H, Karl K, Kandel ER, Hawkins RD. Spontaneous transmitter release is critical for the induction of long-term and intermediate-term facilitation in Aplysia. Proc Natl Acad Sci USA. 2012a; 109:9131–9136. [PubMed: 22619320]

Jin I, Udo H, Rayman JB, Puthanveettil S, Kandel ER, Hawkins RD. Spontaneous transmitter release recruits postsynaptic mechanisms of long-term and intermediate-term facilitation in Aplysia. Proc Natl Acad Sci USA. 2012b; 109:9137–9142. [PubMed: 22619333]

Katz B, Miledi R. Tetrodotoxin-resistant electric activity in presynaptic terminals. J Physiol. 1969a; 203:459–487. [PubMed: 4307710]

Katz B, Miledi R. Spontaneous and evoked activity of motor nerve endings in calcium ringer. J Physiol. 1969b; 203:689–706. [PubMed: 4318717]

Kawasaki F, Collins SC, Ordway RW. Synaptic calcium-channel function in Drosophila: analysis and transformation rescue of temperature-sensitive paralytic and lethal mutations of cacophony. J Neurosci. 2002; 22:5856–5864. [PubMed: 12122048]

Kawasaki F, Felling R, Ordway RW. A temperature-sensitive paralytic mutant defines a primary synaptic calcium channel in Drosophila. J Neurosci. 2000; 20:4885–4889. [PubMed: 10864946]

Kuromi H, Ueno K, Kidokoro Y. Two types of Ca^{2+} channel linked to two endocytic pathways coordinately maintain synaptic transmission at the *Drosophila* synapse. Eur J Neurosci. 2010; 32:335–346. [PubMed: 20704589]

Lee J, Ueda A, Wu CF. Pre- and post-synaptic mechanisms of synaptic strength homeostasis revealed by Slowpoke and Shaker K^+ channel mutations in Drosophila. Neuroscience. 2008; 154:1283–1296. [PubMed: 18539401]

Lee J, Wu CF. Orchestration of stepwise synaptic growth by K^+ and Ca^{2+} channels in Drosophila. J Neurosci. 2010; 30:15821–15833. [PubMed: 21106821]

Leung HT, Branton WD, Phillips HS, Jan L, Byerly L. Spider toxins selectively block calcium currents in Drosophila. Neuron. 1989; 3:767–772. [PubMed: 2642017]

Leung HT, Byerly L. Characterization of single calcium channels in Drosophila embryonic nerve and muscle cells. J Neurosci. 1991; 11:3047–3059. [PubMed: 1658244]

Littleton JT, Ganetzky B. Ion channels and synaptic organization: analysis of the Drosophila genome. Neuron. 2000; 26:35–43. [PubMed: 10798390]

Ly CV, Yao CK, Verstreken P, Ohyama T, Bellen HJ. *Straightjacket* is required for the synaptic stabilization of *cacophony*, a voltage-gated calcium channel α 1 subunit. J Cell Biol. 2008; 181:157–170. [PubMed: 18391075]

Macleod GT, Chen L, Karunanithi S, Peloquin JB, Atwood HL, McRory JE, Zamponi GW, Charlton MP. The Drosophila *cac*^{ts2} mutation reduces presynaptic Ca^{2+} entry and defines an important element in Ca(v)2.1 channel inactivation. Eur J Neurosci. 2006; 23:3230–3244. [PubMed: 16820014]

Marder E, Abbott LF, Turrigiano GG, Liu Z, Golowasch J. Memory from the dynamics of intrinsic membrane currents. Proc Natl Acad Sci USA. 1996; 93:13481–13486. [PubMed: 8942960]

Martin AR. A further study of the statistical composition on the end-plate potential. J Physiol. 1955; 130:114–122. [PubMed: 13278890]

Müller M, Pym ECG, Tong A, Davis GW. Rab3-GAP Controls the progression of synaptic homeostasis at a late stage of vesicle release. Neuron. 2012; 69:749–762. [PubMed: 21338884]

Pauron D, Qar J, Barhanin J, Fournier D, Cuany A, Pralavorio M, Berge JB, Lazdunski M. Identification and affinity labeling of very high affinity binding sites for the phenylalkylamine series of Ca^+ channel blockers in the Drosophila nervous system. Biochemistry. 1987; 26:6311–6315. [PubMed: 2827725]

Paradis S, Sweeney ST, Davis GW. Homeostatic control of presynaptic release is triggered by postsynaptic membrane depolarization. Neuron. 2001; 30:737–749. [PubMed: 11430807]

Pelzer S, Barhanin J, Pauron D, Trautwein W, Lazdunski M, Pelzer D. Diversity and novel pharmacological properties of Ca^{2+} channels in Drosophila brain membranes. Embo J. 1989; 8:2365–2371. [PubMed: 2551681]

Peng IF, Wu CF. Drosophila cacophony channels: a major mediator of neuronal Ca^{2+} currents and a trigger for K^+ channel homeostatic regulation. J Neurosci. 2007; 27:1072–1081. [PubMed: 17267561]

Petersen SA, Fetter RD, Noordermeer JN, Goodman CS, DiAntonio A. Genetic analysis of glutamate receptors in Drosophila reveals a retrograde signal regulating presynaptic transmitter release. Neuron. 1997; 19:1237–1248. [PubMed: 9427247]

Plomp JJ, Van Kempen GThH, Molenaar PC. Adaptation of quantal content to decreased postsynaptic sensitivity at single endplates in α-bungarotoxin-treated rats. J Physiol. 1992; 458:487–499. [PubMed: 1302275]

Rieckhof GE, Yoshihara M, Guan Z, Littleton JT. Presynaptic N-type calcium channels regulate synaptic growth. J Biol Chem. 2003; 278:41099–41108. [PubMed: 12896973]

Ryglewski S, Lance K, Levine RB, Duch C. Ca(v)2 channels mediate low and high voltage-activated calcium currents in Drosophila motoneurons. J Physiol. 2012; 590:809–825. [PubMed: 22183725]

Singh S, Wu CF. Properties of potassium currents and their role in membrane excitability in Dorosphila larval muscle-fibers. J Exp Biol. 1990; 152:59–76. [PubMed: 2121887]

Singh S, Wu CF. Ionic currents in larval muscles of Drosophila. NEUROMUSCULAR JUNCTIONS IN DROSOPHILA Book Series: INTERNATIONAL REVIEW OF NEUROBIOLOGY. 1999; Volume: 43:191–220. Published: 1999.

Smith LA, Wang X, Peixoto AA, Neumann EK, Hall LM, Hall JC. A Drosophila calcium channel alpha1 subunit gene maps to a genetic locus associated with behavioral and visual defects. J Neurosci. 1996; 16:7868–7879. [PubMed: 8987815]

Stewart BA, Schuster CM, Goodman CS, Atwood HL. Homeostasis of synaptic transmission in Drosophila with genetically altered nerve terminal morphology. J Neurosci. 1996; 16:3877–3886. [PubMed: 8656281]

Sudhof TC. The synaptic vesicle cycle. Annu Rev Neurosci. 2004; 27:509–547. [PubMed: 15217342]

Tsien RW, Lipscombe D, Madison DV, Bley KR, Fox AP. Multiple types of neuronal calcium channels and their selective modulation. Trends Neurosci. 1988; 11:431–438. [PubMed: 2469160]

Turrigiano G, LeMasson G, Marder E. Selective regulation of current densities underlies spontaneous changes in the activity of cultured neurons. J Neurosci. 1995; 15:3640–3652. [PubMed: 7538565]

Turrigiano GG, Nelson SB. Homeostatic plasticity in the developing nervous system. Nat Rev Neurosci. 2004; 5:97–107. [PubMed: 14735113]

Ueda A, Wu CF. Distinct frequency-dependent regulation of nerve terminal excitability and synaptic transmission by IA and IK potassium channels revealed by *Drosophila Shaker* and *Shab* mutations. J Neurosci. 2006; 26:6238–6248. [PubMed: 16763031]

Ueda A, Wu CF. Role of *rut* adenylyl cyclase in the ensemble regulation of presynaptic terminal excitability: reduced synaptic strength and precision in a *Drosophila* memory mutant. J Neurogenet. 2009; 23:185–199. [PubMed: 19101836]

von Schilcher F. The behavior of *cacophony*, a courtship song mutant in *Drosophila melanogaster*. Behav Bio. 1976; 17:187–196. [PubMed: 822818]

Worrell JW, Levine RB. Characterization of voltage-dependent Ca^{2+} currents in identified Drosophila motoneurons in situ. J Neurophysiol. 2008; 100:868–878. [PubMed: 18550721]

Yoshihara M, Adolfsen B, Galle KT, Littleton JT. Retrograde signaling by Syt 4 induces presynaptic release and synapse-specific growth. Science. 2005; 310:858–863. [PubMed: 16272123]

Zheng W, Feng G, Ren D, Eberl DF, Hannan F, Dubald M, Hall LM. Cloning and characterization of a calcium channel alpha 1 subunit from Drosophila melanogaster with similarity to the rat brain type D isoform. J Neurosci. 1995; 15:1132–1143. [PubMed: 7869089]

Wu CF, Ganetzky B, Jan LY, Jan YN, Benzer S. Drosophila mutant with a temperature-sensitive block in nerve-conduction. Proc Natl Acad Sci USA. 1978; 75:4047–4051. [PubMed: 211514]

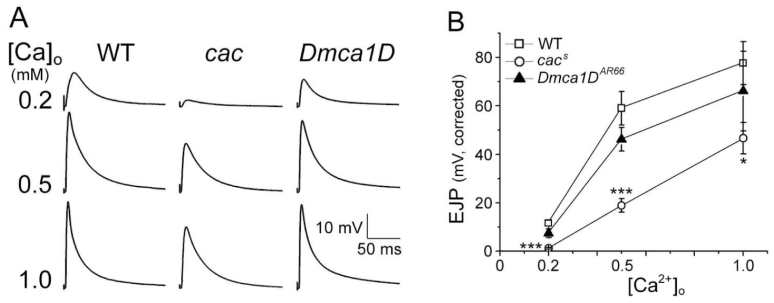

Figure 1.

Altered Ca^{2+} dependency of EJP responses in *cac* mutants. (A) Representative traces of EJPs at different $[Ca^{2+}]_o$ for WT, *cac*, and *Dmca1D* larvae. Note smaller EJPs in *cac* mutants than WT and *Dmca1D* at all $[Ca^{2+}]_o$. (B) Pooled EJP data at different $[Ca^{2+}]_o$ for WT, cac^S, and $Dmca1D^{AR66}$ larvae. EJP amplitude is corrected for nonlinear summation (see Methods). The number of larvae for WT, cac^S, and $Dmca1D^{AR66}$ was 50, 14, and 9 at 0.2 mM Ca^{2+}; 13, 13, and 8 at 0.5 mM Ca^{2+}; 6, 6, and 4 at 1.0 mM Ca^{2+}. Mean ± SEM are indicated. *, P<0.05 and ***, P<0.001, One-way ANOVA with Fisher's LSD test for multiple comparisons.

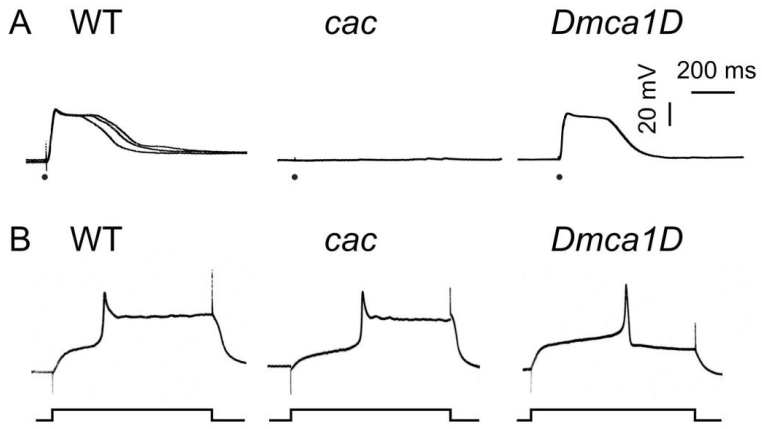

Figure 2.

Preferential functional expression of *cac* and *Dmca1D* Ca^{2+} channels in pre- and post-synaptic sites. (A) Representative traces of EJPs triggered electrotonically in the presence of blockers of Na^{+} (TTX, 3 μM) and K^{+} (4-AP, 200 μM; TEA, 20 mM) channels at a low concentration of external Ca^{2+} (0.1 mM). ● indicates electrotonic stimulation of the nerve terminal (1 ms duration, see Methods). Rare occurrences of plateau EJPs in *cac* indicated weakened Ca^{2+} influx in the presynaptic terminals (see text). WT: 11 out of 11 NMJs (2 larvae of CS and 3 larvae of OR); cac^{s}: 2 out of 8 NMJs ($p < 0.01$; 3 larvae); $Dmca1D^{AR66}$: 4 out of 6 muscles ($p > 0.05$; 3 larvae). Chi-square test with sequential Bonferroni adjustment for multiple comparisons. (B) Representative traces of muscle action potentials triggered by current injection in saline containing 2 mM Sr^{2+}, which partially blocks K^{+} channels and is a more effective charge carrier through muscle Ca^{2+} channels. Shortened muscle action potentials in $Dmca1D^{AR66}$ (5 out of 5 muscles, 2 larvae; $p < 0.001$) in contrast to prolonged Sr^{2+} spikes in WT (10 out of 10 muscles, 8 larvae of CS) indicated weakened Ca^{2+} channel function in the muscle. Prolonged Sr^{2+} spikes were observed in all cac^{S} muscle fibers (9 out of 9 muscles, 3 larvae; $p > 0.05$). Chi-square test with sequential Bonferroni adjustment for multiple comparisons.

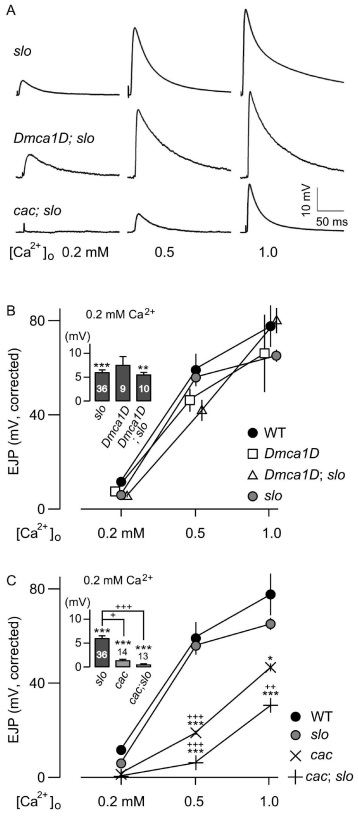

Figure 3.

Effects of *cac* and *Dmca1D* mutations on *slo* EJP amplitude in double-mutant combinations. (A) Representative traces of EJPs at different $[Ca^{2+}]_o$ for *slo*, *cac*^{s}*;;slo*, and *Dmca1D*^{AR66}*;slo* larvae. Note similar response amplitudes between *slo* and *Dmca1D*^{AR66}*;slo* in contrast to smaller EJPs in *cac*^{s}*;;slo*. (B) Pooled EJP data for *Dmca1D*^{AR66}, *slo*, and the double mutants. (C) Pooled EJP data for *cac*^{s}, *slo*, and the double mutants. Note further reduction in EJP amplitudes at different Ca^{2+} levels in *cac*^{s}*;;slo* double mutants compared to *cac* single mutants. EJP amplitudes are corrected for nonlinear summation (see Methods). The insets show at a higher resolution the differences in EJP amplitudes at 0.2 mM $[Ca^{2+}]_o$. Mean ± SEM are indicated. * or $^{+}$, P<0.05, ** or $^{++}$, P<0.01 and *** or $^{+++}$, P<0.001, One-way ANOVA with Fisher's LSD test for multiple comparisons, WT (*) or *slo* ($^{+}$) vs. genotypes indicated.

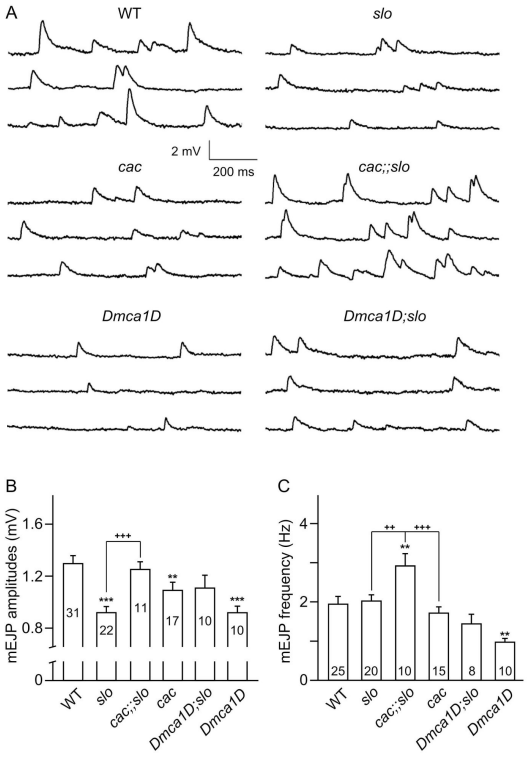

Figure 4.

Effects of *cac* and *Dmca1D* mutations on spontaneous quantal release. (A) Examples of mEJP traces for WT, cac^{S}, $Dmca1D^{AR66}$, *slo*, cac^{S}*;;slo*, and $Dmca1D^{AR66}$;*slo* larvae. (B, C) Pooled data for mEJP amplitude (B) and frequency (C). Note fewer mEJPs in $Dmca1D^{AR66}$ mutants in contrast to more frequent occurrence in cac^{S}*;;slo*, and greater mEJP amplitude in WT and cac^{S}*;;slo* compared to *slo*. The number of larvae is indicated for each genotype. Mean ± SEM. *, P<0.05, ** or $^{++}$, P<0.01 and *** or $^{+++}$, P<0.001, One-way ANOVA with Fisher's LSD test for multiple comparisons, WT (*) vs. other genotypes, or each pair indicated ($^{+}$).

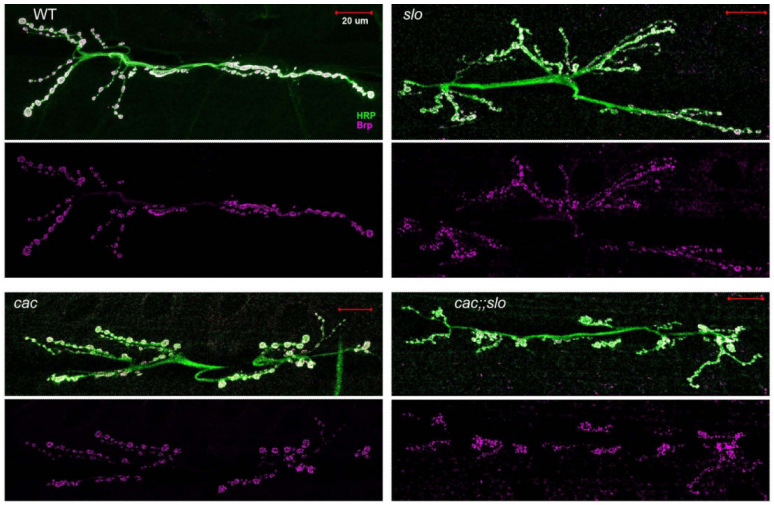

Figure 5.

Gross morphology of NMJs and active zone distribution in *slo*, *cac*, and *cac;slo* mutations. Boutons in *slo* and cac^{S};*slo* exhibited frequent satellite boutons (anti-HRP antibody staining; Lee & Wu, 2010) with active zones (anti-BRP antibody staining). However, no significant alterations in the intensity of anti-BRP staining was observed in *slo*, cac^{S}, and cac^{S};*slo* NMJs compared to WT (cac^{NT27}: 5 NMJs from 2 larvae; cac^{s}: 5 NMJs from 2 larvae; cac^{s};slo^{1}: 6 NMJs from 2 larvae; slo^{1}: 4 NMJs from 2 larvae; WT: 5 NMJs from 3 larvae).

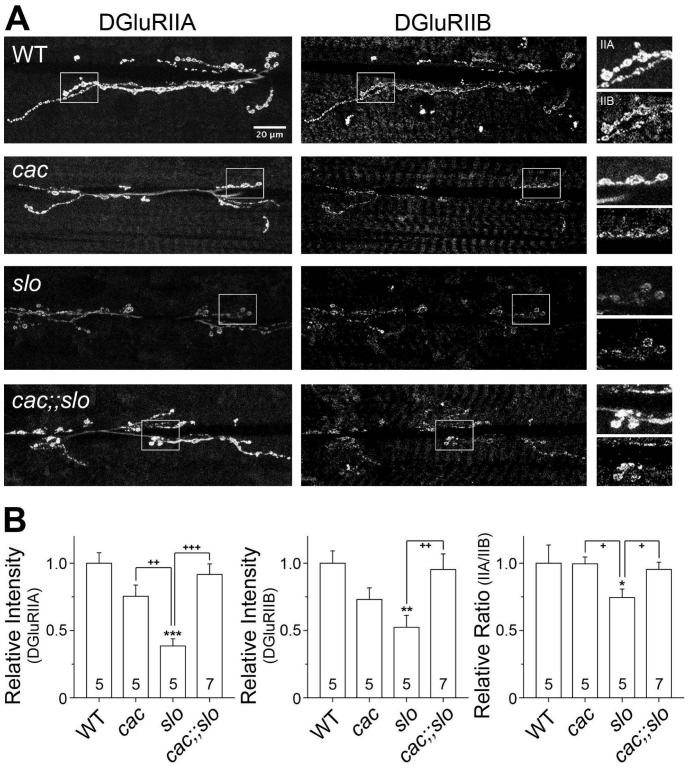

Figure 6.

Effects of *slo*, *cac*, and *cac;;slo* mutations on postsynaptic glutamate receptor density and composition. (A) Relative distributions of postsynaptic DGluRII subunits are shown for each genotype indicated. Note that samples of all genotypes were treated simultaneously throughout the entire immunohistochemical and image analysis procedures (see Methods). Boxed regions in the DGluRIIA and DGluRIIB staining images (two left panels) are magnified twice and presented on the right. Scale bar, 20 μm. (B) Data for the pixel intensity of each DGluRII subunit and their relative ratio are pooled and compared among different genotypes. Note that all values were normalized to that of WT. Mean ± SEM are indicated. * or $^{+}$, P<0.05, ** or $^{++}$, P<0.01 and *** or +++, P<0.001, One-way ANOVA with Fisher's LSD test for multiple comparisons, WT (*) vs. other genotypes, or *slo* ($^{+}$) vs. paired genotypes.

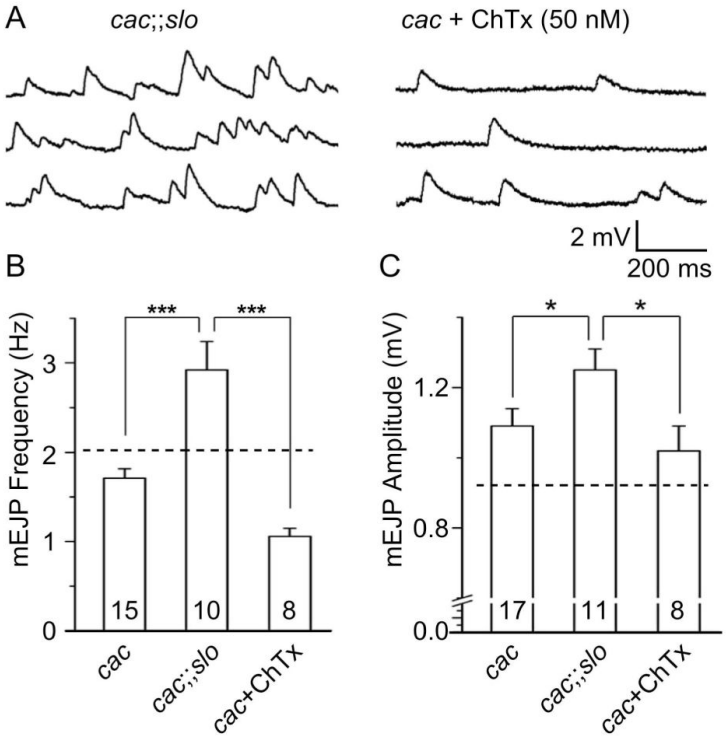

Figure 7.

Lack of acute effects of BK current blockade by ChTx on spontaneous release in *cac* mutants in contrast to striking chronic effects of of BK channel disruption in *cac;;slo* double mutants. (A) Examples of mEJP traces for cac^S*;;slo* double mutants (left) and cac^S mutants treated with ChTx (50 nM). (B, C) Pooled data for mEJP frequency and amplitude. Dashed lines indicate the values for *slo* mutants (cf. Fig. 4). The results of ChTx treatment on cac^S mEJPs are compared with corresponding cac^S and cac^S*;;slo* data (cf. Fig. 4). Note that the phenotype of larger and higher frequency of mEJPs in cac^S*;;slo* could not be reproduced by acute blockade of *slo* BK channels in cac^S mutants. Mean ± SEM are indicated. *, P<0.05 and ***, P<0.001, One-way ANOVA with Fisher's LSD test for multiple comparisons between genotypes paired.

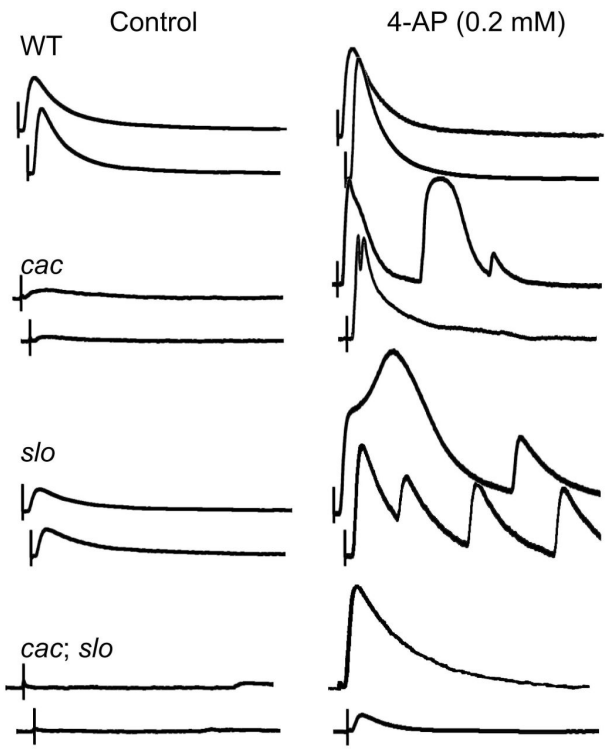

Figure 8.

Altered 4-AP sensitivity of *slo*, *cac*, and *cac;;slo* double mutants. Representative traces of EJP responses before and after a 4-AP treatment (0.2 mM) in WT, *slo*, cac^S, and cac^S*;;slo* larvae. Unlike in WT, selective blockade of Sh I_A by 4-AP in *slo* and cac^S mutants induced prolonged and supernumerary EJPs, indicative of presynaptic hyperexcitability (cf. Lee et al., 2008). In cac^S*;;slo* double mutant larvae, EJPs increased in size significantly but supernumerary EJPs rarely occurred at 0.2 mM 4-AP. Saline contained 0.2 mM Ca^{2+}. Scale bar, 10 mV and 100 ms.

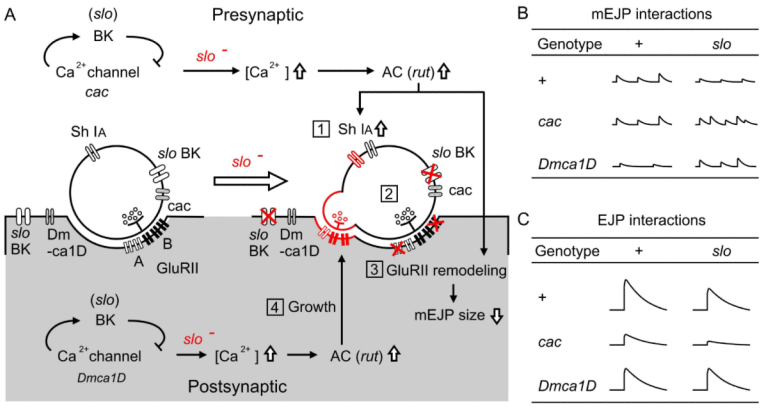

Figure 9.

Summary diagrams for *slo* mutation-induced homeostatic adjustments in synaptic transmission and growth and the potential roles of *cac* and *Dmca1D* in pre- and post-synaptic compartments. (A) The homeostatic adjustments are high-lighted in red and numbered: (1) up regulation of presynaptic Sh channel, (2) unaltered mEJP frequency, (3) decreased mEJP amplitude due to modified postsynaptic DGluRII subunit density and composition, and (4) increased number of satellite bouton growth. The potential roles of *cac* and *Dmca1D* Ca^{2+} channels and their site of action, as well as the *rut* adenylyl cyclase (AC)-mediated adjustments are depicted. (B and C) Modifications in mEJP (B) and EJP (C) amplitudes are summarized for *cac*, *Dmca1D*, *slo*, and their double-mutant combinations.

Table 1

Effects of charybdotoxin (ChTx) on evoked EJPs. EJPs were recorded from the same muscles before and after ChTx (50 nM) treatment. Note that the amplitude and failure rate of EJPs were not significantly affected by ChTx. Data for *cac* is pooled from cac^{S} (n = 2) and cac^{NT27} (n = 3). Mean±SEM are indicated.

Genotype	Before ChTx		After ChTx		n
	ejp (mV)	Failure (%)	ejp (mV)	Failure (%)	
WT	12 ± 1.2	0 ± 0	13 ± 2.7	0 ± 0	5
cac	2.7 ± 0.78	22 ± 5.6	2.4 ± 1.1	36 ± 16	5